STABILITY OF A LAMINAR FLOW ALONG A FLEXIBLE BOUNDARY (III)

TAKEMATSU, Masaki
Research Institute for Applied Mechanics, Kyushu University : Lecturer

https://doi.org/10.5109/7170854

出版情報：Reports of Research Institute for Applied Mechanics. 18 (61), pp.87-100, 1970. 九州大学応用力学研究所
バージョン：

Reports of Research Institute for Applied Mechanics
Vol. XVIII, No. 61, 1970

STABILITY OF A LAMINAR FLOW ALONG A FLEXIBLE BOUNDARY (III)

By Masaki TAKEMATSU*

The stability of a plane laminar flow along a flexible boundary is investigated by a direct numerical method using a digital computor. With the known asymptotic solutions as a guide, machine solutions are sought for moderate or small Reynolds numbers which are beyond the limit of applicability of the asymptotic theory.

Numerical results are presented, together with asymptotic ones, in stability diagrams, which provide a reasonably complete picture of the stability characteristics of the combined fluid-flexible boundary system. There are two distinct families of stability curves; one which forms an island of instability represents the modification of the Tollmien-Schlichting instability, and the other which extends to the inviscid limit does the inviscid types of instability —— the Kelvin-Helmholtz instability clearly belongs in this category ——. Stability curves of the latter family exhibit as well a typical feature of 'free surface waves'. The present investigation tends to confirm the belief that flexible boundaries always destabilize rather than stabilize the boundary-layer flow.

1. Introduction

The stability problem of a laminar flow along a flexible boundary is not only of interest in practical applications; it is also of theoretical interest as a typical example of the composite stability problems which involve two or more distinct types of instability.

Since Kramer's publication[1] on boundary-layer stabilization, this problem has attracted in the past a certain amount of attention[2)~5)]. As far as is known, however, no attempt has been made to give a complete mathematical treatment of the problem.

In a recent paper[6] we have reconsidered this problem with an intention to account for the three possible types of instability directly from a standpoint of ordinary stability theory, and developed an asymptotic method of solution for large Reynolds number. It is demonstrated that not only the Tollmien-Schlichting instability but also such inviscid types of instability as the Kelvin-Helmholtz instability can be accounted for directly by solving asymptotically a

* Lecturer, Research Institute for Applied Mechanics, Kyushu University.

complete viscous eigenvalue problem; somehow this has been passed over by previous authors. A numerical example presented therein indicates that unstable regions of the both types are likely to extend to fairly small Reynolds number. Within the framework of the asymptotic analysis, however, no definite information is obtained as to the third possible type of instability. This type of instability is essentially a resonance effect and may take nearly the same phase velocity as that of free surface waves of the flexible boundary[2]. Landahl[3] has shown that, in fact, this type of instability occurs at rather small Reynolds numbers which are clearly beyond the limits of ordinary asymptotic theories. His calculations are incomplete and correct only qualitatively, so that they illustrate no more than the possible existence of the type of instability. The connection between this and the other types of instability is still an open question.

The purpose of the present paper is to examine the stability characteristics at moderate or smaller (if necessary) Reynolds numbers. This task is feasible only by a direct numerical method. The numerical method employed here is essentially the same as that originally developed by Thomas[7]. For the sake of completeness, we begin with formulation of the problem. Taking the asymptotic results[6] as an indication, computations are extended to smaller Reynolds numbers. A detailed investigation is made especially for a typical flexible boundary which admits the simultaneous existence of the three types of instability. A brief description is also given of the outline of the asymptotic results.

A classical problem closely related to the present one is the generation of Water waves by wind. This problem has been treated by many investigators, though not in any great detail owing to the mathematical complexity involved (cf. e.g. Lock[9], Miles[10),11)]): Miles has conjectured that the third type of instability mentioned above is responsible for the initial formation of water waves, and that the Kelvin-Helmholtz instability is significant for an air-oil interface. It may be interesting to reconsider this problem in the light of the present results.

2. Formulation of the problem

Consider a steady plane parallel flow along a flexible boundary (located at rest at $y=0$) with velocity profile $U(y)$ of the boundary-layer type. We superimpose on this basic equilibrium flow an infinitesimal wave-like disturbance whose stream function has the form

$$\psi(x,\ y,\ t) = \phi(y)e^{i\alpha(x-ct)}, \tag{2.1}$$

where $\alpha\ (>0)$ denotes the wave number in the x-direction, $R_e[c] \equiv c_r$ the phase velocity, and $\alpha I_m[c] \equiv \alpha c_i$ the amplification factor of the disturbance. The perturbation velocities $(u\ ,\ v)$ are then given by

$$u = \psi_y = \phi'\cdot E, \qquad v = -\psi_x = -i\alpha\phi\cdot E, \tag{2.2}$$

where E denotes the $(x\ ,\ t)$-dependence of the disturbance. Substituting (2.2) in the Navier-Stokes equations and neglecting second order quantities, we are led to the well-known Orr-Sommerfeld equation

$$(U-c)(\phi''-\alpha^2\phi)-U''\phi=(i\alpha R)^{-1}(\phi^{\text{iv}}-2\alpha^2\phi''+\alpha^4\phi). \tag{2.3}$$

Here R is the Reynolds number $U_\infty\delta/\nu$ defined by the free-stream velocity U_∞ and the thickness of the boundary-layer δ.

The boundary conditions to be satisfied at infinity are the usual ones, i.e.

$$\phi'(\infty)=\alpha\phi(\infty)=0. \qquad (2.4)_{1,2}$$

The remaining two conditions on $\phi(y)$ are specified at the flexible boundary in motion. Let the normal displacement of the flexible boundary be η, which may be expressed in conformity with (2.1) as

$$\eta(x, t)=\hat{\eta}\cdot E(x, t), \tag{2.5}$$

with the infinitesimal amplitude $\hat{\eta}$. The tangential displacement will be neglected. Hence the kinematical and non-slipping conditions on the boundary are

$$v=\frac{\partial\eta}{\partial t},\qquad u+U=0;\qquad y=\eta(x, t). \tag{2.6}$$

In the linearized approach, these are equivalent to

$$\phi(0)=c\hat{\eta};\qquad \phi'(0)=-U'(0)\hat{\eta}. \tag{2.7}$$

To complete the problem formulation, a dynamical condition relating the normal component (F_n) of the sinusoidal forces exerted by the fluid and the corresponding surface displacement is requisite in addition, which may generally be expressed as

$$Z\eta=F_n, \tag{2.8}$$

by means of a complex stiffness Z. The right-hand side of (2.8) can be evaluated as the sum of the perturbation pressure (p), the normal stress, and the normal component of the tangential stress at the boundary, i.e.

$$F_n=-p+2R^{-1}v_y+R^{-1}U'\eta_x.$$

Within the linear approximation, this can be written as

$$F_n=-\Big[c\phi'(0)+U'(0)\phi(0)+(i\alpha R)^{-1}\{\phi'''(0)-3\alpha^2\phi'(0)+U'(0)\alpha^2\hat{\eta}\}\Big]\cdot E(x, t), \tag{2.9}$$

where p is calculated from the x-momentum equation. Substituting (2.9) in (2.8) and eliminating $\hat{\eta}$ from the resultant equation and (2.7), we have

$$c\phi'(0)+U'(0)\phi(0)=0, \tag{2.10}$$

$$(\alpha R)^{-1}\phi'''(0) - \left[\frac{iZ}{U'(0)} + 4\alpha^2(\alpha R)^{-1}\right]\phi'(0) = 0. \tag{2.11}$$

The Orr-Sommerfeld equation (2.3) together with the four homogeneous boundary conditions $(2.4)_{1,2}$, (2.10) and (2.11) constitute a conventional eigenvalue problem; the usual secular determinant leads to a relation of the form $\Delta(c, \alpha, \alpha R; Z) = 0$. If the mechanical property of the boundary (Z) is specified, then the eigenvalue c can be determined as functions of the real parameters α and αR for a prescribed profile $U(y)$. The criterion for stability is that $I_m[c] < 0$, while if $I_m[c] > 0$ the flow together with the boundary is unstable.

For numerical examples we consider a rather simple flexible boundary characterized by an effective mass (m), a damping coefficient (κ) and a free wave velocity ($\bar{a}$). In this case, the complex stiffness Z takes the following form

$$Z = M\alpha^2(a^2 - c^2) - i\alpha cK, \tag{2.12}$$

where M, a and K are dimensionless parameters defined respectively by

$$M = m/(\rho\delta),\ a = \bar{a}/U_\infty \text{ and } K = \kappa/(\rho U_\infty).$$

For numerical solution of the problem, it is particularly convenient to divide the whole flow field into two regions; i.e. the outer region, say $y > y_0$, where the basic flow is supposed to be substantially constant and the inner region. At the boundary point $y = y_0$ of the two regions, however, the following matching conditions must be fulfilled:

$$[\phi] = [\phi'] = [\phi''] = [\phi'''] = 0, \tag{2.13}$$

the symbol $[\phi]$ being used for $\lim_{\varepsilon \to 0}[\phi(y_0+\varepsilon) - \phi(y_0-\varepsilon)]$. In the outer region, the Orr-Sommerfeld equation (2.3) simplifies to

$$\left(\frac{d^2}{dy^2} - \alpha^2\right)\left(\frac{d^2}{dy^2} - \gamma^2\right)\phi = 0, \tag{2.14}$$

where

$$\gamma = \{\alpha^2 + i\alpha R(1-c)\}^{1/2}. \tag{2.15}$$

Then if we choose $R_e[\gamma] > 0$, the general outer-region solution satisfying the boundary conditions at infinity $(2.4)_{1,2}$ can be written as

$$\phi = A_1 e^{-\alpha y} + A_2 e^{-\gamma y}, \tag{2.16}$$

where the A's are unknown coefficients. Substituting (2.16) in (2.13) and eliminating the A's from the resultant expressions, we have the following two boundary conditions for the inner-region solution:

$$\left.\begin{aligned} &\phi''(y_0) + (\alpha + \gamma)\phi'(y_0) + \alpha\gamma\phi(y_0) = 0, \\ &\phi'''(y_0) + \gamma\phi''(y_0) - \alpha^2\phi'(y_0) - \alpha^2\gamma\phi'(y_0) = 0. \end{aligned}\right\} \tag{2.17}$$

Now that the behaviour of the outer-region solution has been replaced by the above two conditions, we are only to deal with the finite inner-region under the boundary conditions (2. 10), (2. 11) and (2. 17).

3. Numerical solution of the eigenvalue problem

***Finite difference techniqne*:** To obtain machine solutions, we now replace the continuous problem in differential form by finite difference approximations. We subdivide the inner-region $0 \leqq y \leqq y_0$ into n intervals and let h $(= y_0/n)$ be the increment in y. The value of ϕ at $y = jh$ is then labeled ϕ_j. If h is small enough, derivatives may be expressed in central differences of the discrete

$$\begin{bmatrix} \phi_j \\ h\phi_j' \\ h^2\phi_j'' \\ h^3\phi_j''' \\ h^4\phi_j^{\mathrm{iv}} \end{bmatrix} = \begin{bmatrix} 0 & 0 & 1 & 0 & 0 \\ 0 & -\frac{1}{2} & 0 & \frac{1}{2} & 0 \\ 0 & 1 & -2 & 1 & 0 \\ -\frac{1}{2} & 1 & 0 & -1 & \frac{1}{2} \\ 1 & -4 & 6 & -4 & 1 \end{bmatrix} \begin{bmatrix} \phi_{j-2} \\ \phi_{j-1} \\ \phi_j \\ \phi_{j+1} \\ \phi_{j+2} \end{bmatrix} + \begin{bmatrix} O(h^2) \\ O(h^2) \\ O(h^2) \\ O(h^2) \\ O(h^2) \end{bmatrix}, \tag{3.1}$$

variable* as the truncation errors being of order h^2. According to Thomas[7], the truncation errors can be reduced to $O(h^4)$ on all derivatives except the third derivative by introducing the new independent variable

$$g = \left(1 - \frac{1}{6} h^2 \frac{d^2}{dy^2} + \frac{1}{90} h^4 \frac{d^4}{dy^4}\right) \phi. \tag{3.2}$$

In the present case when the third derivative appears in the boundary conditions, the transformation (3.2) can not necessarily be expected to be effective. Nevertheless, we shall adopt the transformation because it may scarcely affect the machine time. In terms of g the derivatives are expressed as follows:

$$\begin{bmatrix} \phi_j \\ h\phi_j' \\ h^2\phi_j'' \\ h^3\phi_j''' \\ h^4\phi_j^{\mathrm{iv}} \end{bmatrix} = \begin{bmatrix} \frac{1}{360} & \frac{7}{45} & \frac{41}{60} & \frac{7}{45} & \frac{1}{360} \\ 0 & -\frac{1}{2} & 0 & \frac{1}{2} & 0 \\ \frac{1}{12} & \frac{2}{3} & -\frac{3}{2} & \frac{2}{3} & \frac{1}{12} \\ -\frac{1}{2} & 1 & 0 & -1 & \frac{1}{2} \\ 1 & -4 & 6 & -4 & 1 \end{bmatrix} \begin{bmatrix} g_{j-2} \\ g_{j-1} \\ g_j \\ g_{j+1} \\ g_{j+2} \end{bmatrix} + \begin{bmatrix} O(h^4) \\ O(h^4) \\ O(h^4) \\ O(h^4) \\ O(h^4) \end{bmatrix}. \tag{3.3}$$

Applying (3.3) to the Orr-Sommerfeld equation at each grid point, we have

* cf. e.g. Booth[8]

$$Q_2^j g_{j-2} + Q_1^j g_{j-1} + Q_0^j g_j + Q_1^j g_{j+1} + Q_2^j g_{j+2} = 0, \tag{3.4}$$

where

$$Q_2^j = 1 - \frac{h^2}{12}(\alpha^2 + E_j) + \frac{h^4}{360}(\alpha^2 E_j + i\alpha R U_j''),$$

$$Q_1^j = -4 - \frac{2}{3}h^2(\alpha^2 + E_j) + \frac{7}{45}h^4(\alpha^2 E_j + i\alpha R U_j''),$$

$$Q_0^j = 6 + \frac{2}{3}h^2(\alpha^2 + E_j) + \frac{41}{60}h^4(\alpha^2 E_j + i\alpha R U_j''),$$

$$E_j = \alpha^2 + i\alpha R(U_j - c), \qquad U_j \equiv U(hj).$$

Similarly, the boundary conditions (2.10) and (2.11) at the boundary are reduced to

$$\left.\begin{aligned} B_{11}g_{-2} + B_{12}g_{-1} + B_{13}g_0 + B_{14}g_1 + B_{15}g_2 = 0, \\ B_{21}g_{-2} + B_{22}g_{-1} + B_{23}g_0 + B_{24}g_1 + B_{25}g_2 = 0, \end{aligned}\right\} \tag{3.5}$$

and the matching conditions (2.17) at $y = y_0$ are

$$\left.\begin{aligned} \hat{B}_{11}g_{n-1} + \hat{B}_{12}g_n + \hat{B}_{13}g_{n+1} + \hat{B}_{14}g_{n+2} + \hat{B}_{15}g_{n+3} = 0, \\ \hat{B}_{21}g_{n-1} + \hat{B}_{22}g_n + \hat{B}_{23}g_{n+1} + \hat{B}_{24}g_{n+2} + \hat{B}_{25}g_{n+3} = 0. \end{aligned}\right\} \tag{3.6}$$

The B's and $\hat{B}$'s are given in the Appendix.

The continuous problem has now been reduced to a set of linear homogeneous algebraic equations, for which a non-trivial solution exists only if the determinant of the coefficient matrix vanishes; i.e.

$$D(c, \alpha, \alpha R; Z) = 0. \tag{3.7}$$

The eigenvalues are then determined as the zeros of the determinant which is developed also in the Appendix.

***Technique for obtaining eigenvalues*:** The task is now to determine such combitations of the stability parameters α, αR and c that make the determinant (A. 1) zero for a prescribed velocity profile $U(y)$ and mechanical property of the boundary. In the present approach, a trial-and-error numerical method was used.

For each choice of α and αR, the determinant values were computed at appropriate grid points in the complex c-plane. A possible location of a zero in the complex c-plane was then determined by interpolation from those determinant computations*. The search for zeros was initiated from the region of large αR where possible eigenvalues can be guessed with fair accuracy by

* In cases when c_i and α or αR were chosen arbitrarily, the search for zeros was carried out in the $(c_r - \alpha R)$ or $(c_r - \alpha)$ plane.

means of the asymptotic theory developed in a previous paper[6].

For the computations of the determinant (generally of large size), the sweeping out method was used; in passing we note that this is essentially equivalent to solving the set of linear equations (3.4), (3.5) and (3.6) by an elimination method. Exploiting the peculiar form of the matrix such that non-zero elements are concentrated only in the vicinity of the main diagonal, we designed an efficient computor program which does not operate on zero elements. To secure a sufficient digit accuracy in the final results, about 18 decimal digits were retained in all the computations (double precision computation). The increment h in the independent variable y (i.e. the size of the matrix) was selected in each computation tentatively with reference to the analytical nature of the Orr-Sommerfeld equation. The question of whether those selected values of h (n) were small (large) enough was settled *a posteriori* by spot checks.

4. Results and concluding remarks

In all the numerical examples presented below, we take

$$U(y) = \tanh(2y), \tag{4.1}$$

as a model of velocity profiles of the boundary-layer type. Then the resulting stability characteristics may differ quantitatively from those for the exact Blasius profile*. So far as their essential aspects are concerned, however, they are expected to be true also of various other profiles of the boundary-layer type including the exact Blasius profile.

Asymptotic results : Before presenting the results of numerical solution, it may be well to give here an outline of the asymptotic results which are obtained by means of the procedure proposed in the previous paper[6].

As is readily seen from (2.8), the familiar case of a rigid boundary is included in the present problem formulation as a limiting case of $|Z| \to \infty$. In particular for the type of flexible boundary whose mechanical property is given as (2.12), formally two limit processes are possible in going over to the case of a rigid boundary; i.e. M (or a^2) $\to \infty$ or $K \to \infty$. Numerical examples shown in Fig. 1, 2 and 3 are intended to illustrate the change in stability characteristics to these extreme cases. The curve for a rigid wall is also included in each figure for purpose of comparison. In Fig. 1 and 2 which have relatively large mass-ratios and a small damping, there appear two stability loops (A) and (B). The loop (B) of the inviscid type is largely independent of the Reynolds number and is apparently indicative of the Kelvin-Helmholtz wave. On the other

* Recently Gotoh[12] has shown that in the case of a rigid wall, the particular profile (4.1) results in a considerably larger critical Reynolds number than that for the Blasius profile.

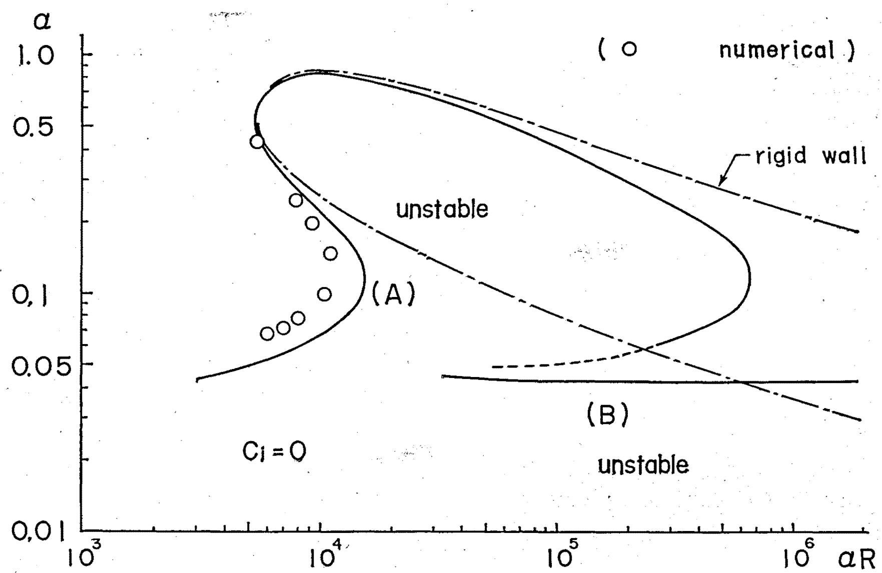

Fig. 1. Neutral stability curves: $M=30$, $K=0.05$, $a^2=0.5$.

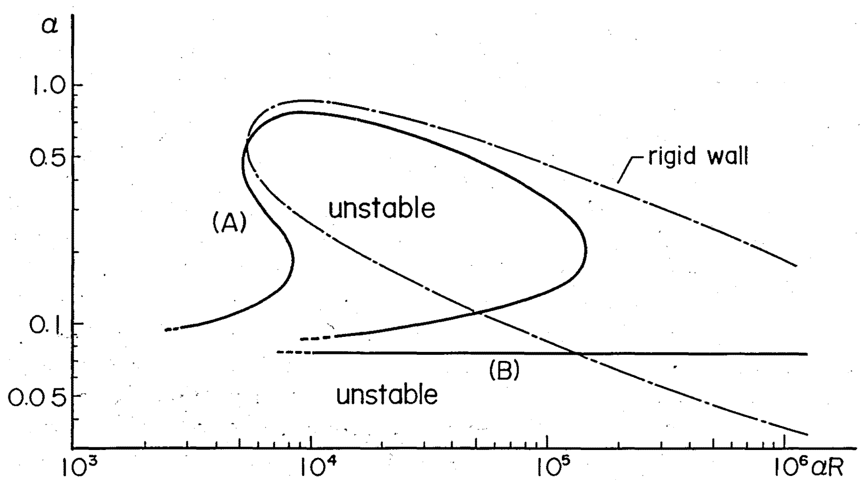

Fig. 2. Neutral stability curves: $M=15$, $K=0.05$, $a^2=0.5$.

hand, the loop (A) represents the modification of the Tollmien-Schlichting wave. So long as α is not too small, this loop shows the same trend as the corresponding one for a rigid wall. However, as α (and hence $|Z|$) decreases to approach a value at which the other instability may occur, it assumes a quite different feature; the both branches of the loop take certain maximum values of αR and then turn back to smaller αR rather than extend to infinity. If M is increased

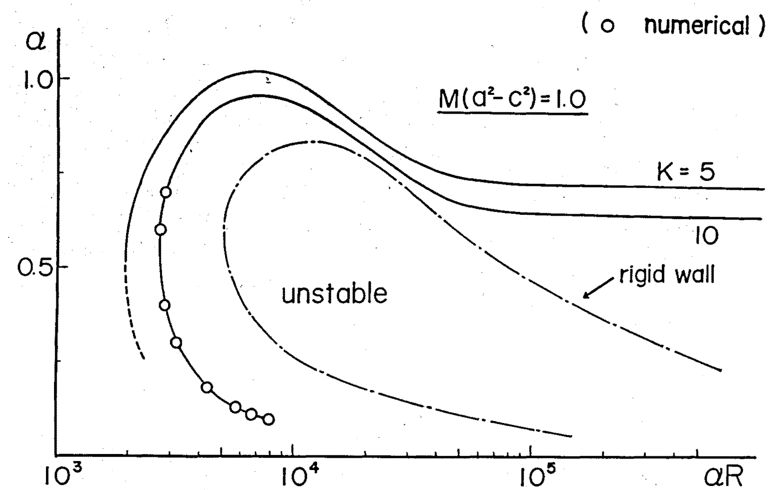

Fig. 3. Neutral stability curves.

with K kept small, the two 'turning points' of the loop (A) move to larger αR along the curve for a rigid wall and the loop (B) shifts parallel to smaller α. In the extreme case of $M \to \infty$, the loop (A) coincides with the one for a rigid wall, while the loop (B) degenerates to the αR axis. To the contrary if we choose M smaller and K larger, the unstable region enclosed by the loop (B) expands to larger α, while the loop (A) shrinks. Eventually the loop (A) disappears completely and there remains only one loop of the inviscid type as (B). This is illustrated in Fig. 3. In the figure $M(a^2-c^2)$ is chosen as a parameter for convenience. For such large values of K, however, the stability curves are rather insensitive to changes in the parameter and furthermore c^2 is very small (<0.1) along the curves, so that the stability curves in Fig. 3 can be interpreted approximately as those for fixed values of M and a^2, say $M \simeq 2$ and $a^2 \simeq 0.5$. As K is increased, the loop approaches the one for a rigid wall. From these figures it may be seen that the flexible boundary of the type under consideration alway destabilize the boundary-layer flow. Further we note that within the framework of the asymptotic theory, the stability diagrams in these figures cannot be completed so successfully as in the case of a rigid wall.

Now it is obvious that those asymptotic results must be complemented by means of the direct numerical method. For the particular velocity profile (4.1), the outer edge of the inner region was taken to be $y_0=1.5$; that is, the matching conditions (2.17) were applied at $y=1.5$. Fig. 4 shows an example of the trend of c_r and αR with increasing determinant size for a particular value of c_i and α. From the figure we can see whether the selected value of the increment h in y ($h=1.5/n$) was small enough. Similar spot checks were made properly in the course of the computation.

As illustrated in Fig. 3, a flexible boundary with extremely large damping has a rather simple stability curve. We are only to examine its 'lower branch' numerically; along the 'lower branch', the important parameter $c(\alpha R)^{1/3}$ becomes too small for the asymptotic method to determine the 'lower branch' correctly. Results of computation for $K=10$ are already plotted in Fig. 3.

For such combinations of the boundary parameters as used in Fig. 1 and 2, the stability characteristics are rather complicated and unfamiliar as compared with those found thus far in other stability problems. It is of particular interest not only to check those asymptotic results but also to extend them to smaller values of αR. The numerical results plotted together in Fig. 1 are intended to confirm the seemingly odd behaviour of the branch of the loop (A). A more extensive computation was carried out for the same combination of the boundary parameters as used in Fig. 2. The results are plotted in Fig. 5 together with the asymptotic ones. Some of partial cross plots of Fig. 5 are presented in Fig. 6 and 7 (in Fig. 7 are shown only the eigenvalues related to the loop (A)). From these cross plots, it is clearly seen that the loop (A) forms an island of instability. The lower branch (with smaller α) of the curve (B_1) was located according to the indication of the asymptotic result. Although there is some discrepancy*, this branch seems to be the counterpart of (B). Tracing this branch carefully in the direction of smaller αR, we found out the upper branch (with larger α) of (B_1), and then a detailed cross examination at $\alpha R=10^3$

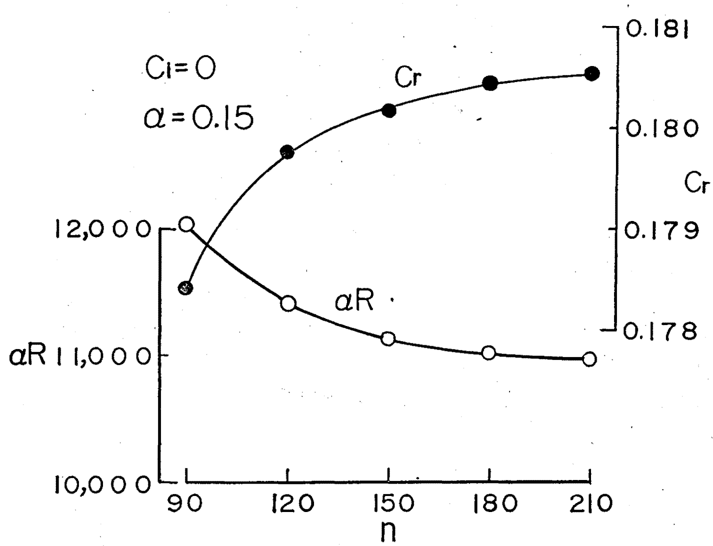

Fig. 4. Trend of αR and c_r with increasing size of the matrix.

* The discrepancy may be due to the inaccuracy of the graphical method employed in solving the asymptotic eigenvalue equation. This may be true also of the results in Fig. 1.

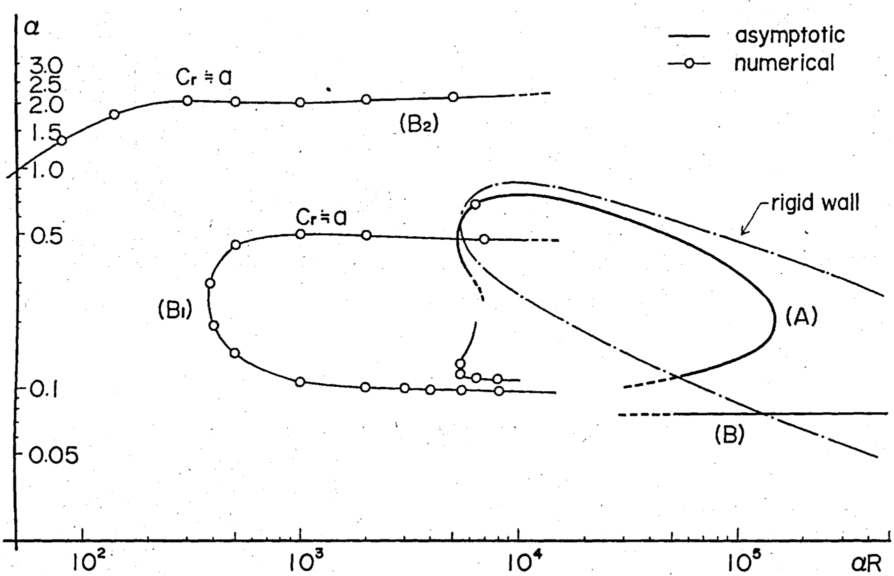

Fig. 5. Neutral stability curves: $M=15$, $K=0.05$, $a^2=0.5$.

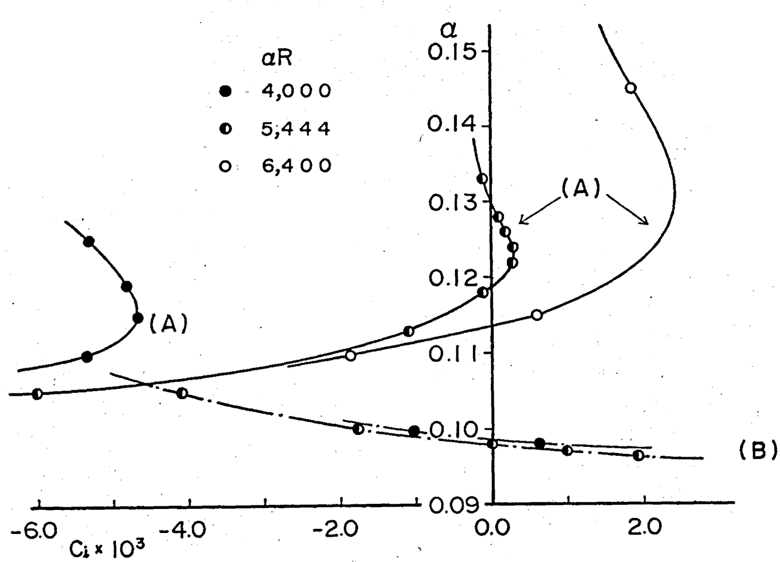

Fig. 6. Cross plots of Fig. 1 at three values of αR.

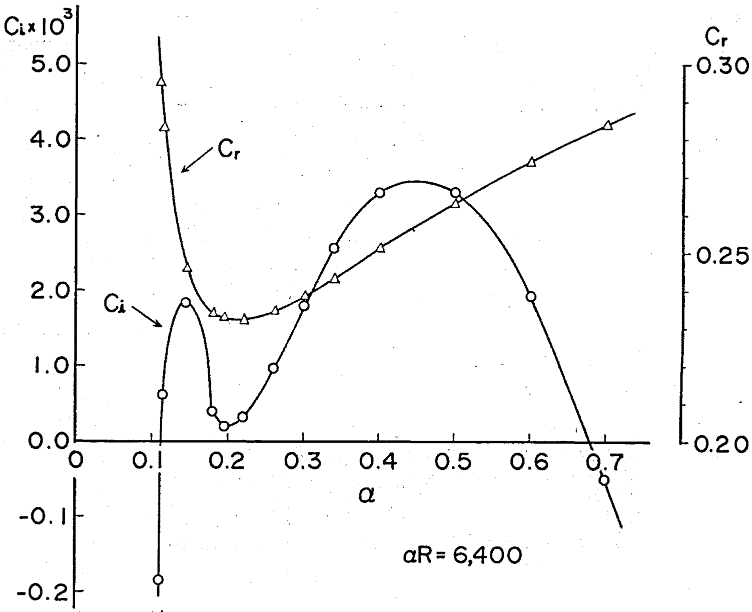

Fig. 7. Cross plot of the unstable domain (A) of Fig. 1.

revealed the existence of the curve (B_2); of course (B_2) belongs to the same family of stability curves as (B_1). Without the indication of the asymptotic results, these branches would be missed. Now it should be emphasized that along both the curve (B_2) and the upper branch of (B_1) the phase velocity c_r of the disturbances is much the same as the propagation speed a of free surface waves of the boundary. The disturbances described by these branches are then identified with 'free surface waves' mentioned in the introduction. These branches may possibly extend to the inviscid limit. In fact, the possible existence of the corresponding inviscid eigenvalues can be seen, though vaguely, from the inviscid eigenvalue equation. For larger values of K, however, the inviscid eigenvalue equation has obviously no solution with $c_r \simeq a$; it is conjectured that in this case (B_1) and (B_2) join together at a finite value of αR. For the combination of the boundary parameters used in Fig. 5, the critical Reynolds number is of order 1.

Throughout this study we have assumed that the flexible boundary is not free to move in its own plane. Hence the present problem formulation is applicable only to a flexible, yet still solid boundary and to the air-oil interface where surface current can effectively be neglected. As for numerical examples, we have considered only a restricted type of flexible boundaries whose mechanical properties are expressed as (2.12). However, the essential features of the three types of instability illustrated in Fig. 5 may be true also of other various boundaries. As far as is known, this is the first time that 'free surface waves' has ever been definitely described in practice.

The author wishes to express his cordial thanks to Professor Tamada K., Doctor Yamada H. and Professor Sakurai T. for their advice, guidance and helpful suggestions during the course of this work and to Doctor Gotoh K. for his constructive criticism and personal interest. Thanks are also due to Professor Okabe J. for his continual encouragement and interest throughout this work. For numerical computations and preparation of the manuscript assistances have been given by Mr. Yamashita I. and Miss Itoh M., to whom the author is much obliged. The computing was performed on the FACOM 230-60 machines of Kyushu University and Kyoto University. This paper is a part of the dissertation submitted by the author to Kyoto University in partial fulfilment of the requirements for the degree of Doctor of Engineering.

References

1) Kramer, M. O., J. Amer. Soc. Nav. Engrs., vol. 72, 1960, pp. 25-33.
2) Benjamin, T. B., J. Fluid Mech., vol. 9, 1960, pp. 513-532.
3) Landhal, M. T., J. Fluid Mech., vol. 13, 1961, pp. 609-632.
4) Hains, F. D., AIAA J., vol. 3, 1965, pp. 775-776.
5) Betchov, R., *Stability of Parallel Flow*, Academic Press, 1967, pp. 233-245.
6) Takematsu, M., Rep. Res. Inst. Appl. Mech., vol. 17, no. 56, 1969, pp. 25-37.
7) Thomas, L. H., Phys. Rev., vol. 91, no. 4, 1953, pp. 780-783.
8) Booth, A. D., *Numerical Methods*, Butterworth, 1966.
9) Lock, R. C., Proc. Camb. Phil. Soc., vol. 50, 1954, pp. 105-124.
10) Miles, J. W., J. Fluid Mech., vol. 3, 1957, pp. 185-204.
11) Miles, J. W., J. Fluid Mech., vol. 6, 1959, pp. 583-598.
12) Gotoh, K., J. Phy. Soc. Japan, vol. 28, no. 3, 1970, pp. 780-783.

(Received July 25, 1970)

Appendix

The coefficients of g's in (3.4), (3.5) and (3.6) form the following determinant: $D(c, \alpha, R; Z)$

$$
= \begin{vmatrix}
B_{11} & B_{12} & B_{13} & B_{14} & B_{15} & 0 & 0 \cdots & & & & & \cdots 0 \\
B_{21} & B_{22} & B_{23} & B_{24} & B_{25} & 0 & 0 \cdots & & & & & \cdots 0 \\
Q_2^0 & Q_1^0 & Q_0^0 & Q_1^0 & Q_2^0 & 0 & 0 \cdots & & & & & \cdots 0 \\
0 & Q_2^1 & Q_1^1 & Q_0^1 & Q_1^1 & Q_2^1 & 0 \cdots & & & & & \cdots 0 \\
0 & 0 & Q_2^2 & Q_1^2 & Q_0^2 & Q_1^2 & Q_2^2 \; 0 \cdots & & & & & \cdots 0 \\
& \cdots\cdots & & & \cdots\cdots & & & \cdots\cdots & & & & \cdots\cdots \\
0 \cdots & & & & & & 0 & Q_2^{n+1} & Q_1^{n+1} & Q_0^{n+1} & Q_1^{n+1} & Q_2^{n+1} \\
0 \cdots & & & & & & 0 & \hat{B}_{11} & \hat{B}_{12} & \hat{B}_{13} & \hat{B}_{14} & \hat{B}_{15} \\
0 \cdots & & & & & & 0 & \hat{B}_{21} & \hat{B}_{22} & \hat{B}_{23} & \hat{B}_{24} & \hat{B}_{25}
\end{vmatrix} = 0 . \quad \text{(A.1)}
$$

Here Q's are given below (3.4), and

$$\begin{cases} B_{11} = \frac{1}{360}U'(0)h, & B_{21} = 1, \\ B_{12} = -\frac{1}{2}c + \frac{7}{45}U'(0)h, & B_{22} = -2 - h^2\left(\frac{i\alpha RZ}{U'(0)} + 4\alpha^2\right), \\ B_{13} = \frac{41}{60}U'(0)h, & B_{23} = 0, \\ B_{14} = \frac{1}{2}c + \frac{7}{45}U'(0)h, & B_{24} = -B_{22}, \\ B_{15} = B_{11}, & B_{25} = -1.0 \ . \end{cases}$$

$$\hat{B}_{11} = \frac{1}{12} + \frac{1}{360}\alpha\gamma h^2,$$

$$\hat{B}_{12} = \frac{2}{3} - \frac{1}{2}h(\alpha + \gamma) + \frac{7}{45}\alpha\gamma h^2,$$

$$\hat{B}_{13} = -\frac{3}{2} + \frac{41}{60}\alpha\gamma h^2,$$

$$\hat{B}_{14} = \frac{2}{3} + \frac{1}{2}h(\alpha + \gamma) + \frac{7}{45}\alpha\gamma h^2,$$

$$\hat{B}_{15} = \hat{B}_{11},$$

$$\hat{B}_{21} = -\frac{1}{2} + \left(\frac{1}{12} - \frac{1}{360}\alpha^2 h^2\right)\gamma h,$$

$$\hat{B}_{22} = 1 + \frac{1}{2}\alpha^2 h^2 + \left(\frac{2}{3} - \frac{7}{45}\alpha^2 h^2\right)\gamma h \ ,$$

$$\hat{B}_{23} = -\left(\frac{3}{2} + \frac{41}{60}\alpha^2 h^2\right)\gamma h,$$

$$\hat{B}_{24} = \hat{B}_{22} - 2\alpha^2 h^2,$$

$$\hat{B}_{25} = \hat{B}_{21} + 1 \ .$$